Multicomponent Plasma Distributions in the Tail Current Sheet Associated with Substorms

LiJen Chen,[1,2] D. Larson,[3] R. P. Lin,[3] M. McCarthy,[2] and G. Parks[2]

Abstract. The 3D plasma instrument on the Wind spacecraft has obtained new features of plasma distributions in the region of the geomagnetic tail current sheet (CS) that have not been previously reported. In addition to the isotropic plasma sheet component, ion beams of energy 1-3 keV are observed. The beams are generally counter streaming but unidirectional beams are also observed streaming parallel and antiparallel to the direction of the magnetic field. In addition, a low energy (a few hundred eV) ion component appears in close association with B_z increases. The electron distributions have bidirectional anisotropy with $T_{\|}/T_{\perp} \approx 1.5$, and they are often accompanied by counter streaming beams. However, a few keV unidirectional electron beam is also observed with bidirectional anistoropic distributions. These keV electrons are streaming away from the CS, suggesting they have been accelerated in the CS and subsequently ejected. The plasma distribution in the CS is multicomponent and thus requires a kinetic description of the dynamics.

Introduction

It is known that Earth's magnetic tail supports a current sheet (CS) and during substorms this CS undergoes a major reconfiguration which dramatically changes the global geomagnetic field topology. Substorms are accompanied by numerous particle and field disturbances that include , for example, auroral expansion (Akasofu, 1968), injection and precipitation of particles (Parks and Winckler, 1968), fluctuation of magnetic field in the plasma sheet (Lui et al., 1992), and a host of other effects (see Kokubun and Kamide, 1998). However, the physics of how these features are related to the dynamics of the CS is not understood.

Studying the behavior of plasma distributions in the region of the CS can yield important information on the dynamics of substorms. Although numerous studies have been made of the plasma in the plasma sheet boundary layer (see Parks et al., 1998 and references therein), only few papers have addressed the behavior in the vicinity of the central plasma sheet (CPS) and the CS. The work of Hada et al. (1981) shows that electron distributions in the plasma sheet (PS) have bidirectional pitch-angle anisotropy and inside $\approx$10 R_e,

sharply field-aligned counter streaming beams exist. Nakamura et al. (1992) studied ion distributions in the vicinity of the neutral sheet and showed that ion distributions consist mostly of a single plasma component and, more recently, Frank et al. (1996) showed ions in the CPS are field-aligned and traveling toward the tail.

The purpose of this article is to present new data obtained by our Wind 3D plasma instrument (Lin et al., 1995) not previously reported or discussed. Our observations come during the perigee passes in the geomagnetic tail when Wind traversed the vicinity of the CPS and CS. We will show that the plasma in the CS region consists of several components for both ions and electrons.

Observations

The neighborhood of the CS is identified by the reversal of the Bx component and/or a high magnetic elevation angle, $|\theta = \sin^{-1}(B_z/|\mathbf{B}|)| > \mathbf{30}^\circ$. The measured magnetic field is a superposition of Earth's dipole field and the field produced by the CS. Towards the middle of the CS, B_x becomes vanishingly small and Earth's dipole field dominates, that is, B_z dominates or it is one of the dominating components.

The top three panels of Figure 1 show the behavior of the three moments (density, mean velocity, mean standard deviation of the velocity) of ion distributions observed on May 10, 1996 for the time interval 0330-0500 UT. These moments are computed for $\approx$ 80 eV - 27 keV ions using data that have been averaged over 24s. The fourth panel shows 3s averages of the magentic field data (courtesy of R. Lepping), and the bottom two panels, energy-time spectrograms of ions travelling in the sunward and antisunward directions. The GSM position of Wind at 0430 UT was (-12 , 6 , 2) in earth-radii (R_e).

The onset of a substorm occurred at $\sim$0400 UT as observed by Canopus magnetometers (not shown). Until about 04 UT, one can deduce from the large B_x that Wind was in the vicinity of the PSBL. Spectrograms show presence of $<$ 10 keV beams for both sunward and tailward ions. An intense low energy component ($<$ 1 keV) is observed for only the tailward going particles. The counter streaming beams that are unbalanced and the presence of the low energy component only in the tailward direction result in net sunward mean velocities that reach several hundred km/s. From $\sim$ 04 UT, Wind was at the edge of PSBL boundary for $\sim$ 7 minutes, as evidenced by the weaker but persistent earthward flux, and then returned to the PS. A series of small B_z increases (dipolarizations) then followed.

At $\sim$ 0426 UT when B_z increased from $\sim$5 nT to 19 nT, the spacecraft was in the CS region characterized by a density of $\approx$0.2/cc and magnetic field intensity $\approx$15 nT with and elevation angle fluctuating between 30°-60°. This B_z increase was accompanied by high frequency magnetic field variations and a large mean velocity, $\approx$800 km/s produced by enhanced ion fluxes with energies from $\approx$2 keV to $>$ 27 keV in the sunward direction and reduced ion fluxes in the tailward direction. The spacecraft remained in the CS past 05 UT.

To illustrate the phase space characteristics of the keV beams in the plasma distributions, we show in Figure 2, first and third rows, examples of 3D distributions of ions and electrons projected on the plane whose normal is defined by $\mathbf{B}\times\mathbf{V}$, where $\mathbf{V}$ is the mean velocity, with $\hat{B}$ as X-axis and $\hat{V}_\perp$ as Y-axis. The date, start and end times when the distributions were obtained are shown on the top. The magnetic elevation angle is shown on the top left, the azimuth on the top right, and the field intensity on the lower right corner. The color lines are isocontours of phase space densities in $(V_\parallel, V_\perp)$ space. The second and fourth rows show 1D cuts of the distributions along parallel ($\times$) and perpendicular ($\diamondsuit$) directions where the solid line denotes the instrument background level. The electron distributions are 3s averages and transmitted every 50s, while the ions are 24s averages. The magnetic field data used are 3s averages for electrons and 24s for ions.

At 0432:19 UT, the ion distribution consisted of nearly circular isotropic contours for V$>$1000 km/s, flatter and less smooth contours for negative Vs due to reduced fluxes of ions from that direction. A weak beam at V$\approx$500 km/s is propagating along the direction parallel to B. The electrons are anisotropic with more electrons along B than perpendicular to B and there is also a weak beam propagating along B at $\approx 2\times10^4$ km/s. Both of the beams are travelling away from the CS. Note that B_x is positive and so the spacecraft is above the CS. Therefore, the direction parallel to B means away from the CS.

The CS is dynamic. At 0435:16 UT, three minutes later, we see the nearly same distribution for the energetic ions but the ion beam at 500 km/s is no longer there. Instead, we see a new beam at -550 km/s propagating in the antiparallel direction to B. The electron distribution did not change significantly and still showed anisotropy and a weak beam but now at slightly less V ($\approx 1.5\times10^4$ km/s) than before. Note that the ion and electron beams are propagating in the opposite direction, that is, the electrons away from the CS and

the ions toward the CS.

The last example which comes ≈15 minutes later at 0450:28 UT, shows again a similar distribution for the energetic ions but now with counter streaming ion beams at V≈400 km/s along B and -700 km/s antiparallel to B. The electrons still show bidirectional anisotropy, which is typical of electron distributions in the CS [Hada et al. 1981], and there are no beams.

Figure 3 shows another example from September 8, 1997. At 1630 UT, the spacecraft was located in GSM coordinates (-13, 7, 1)R_e. and a substorm expansion was observed by the IMAGE magnetometer chain (not shown)at the same time. The format here is the same as before. On this day, the spacecraft was in the southern hemisphere (negative B_x) and it was in the lobe (nearly zero flux) from ≈ 16 UT to 1630 UT. Intense fluxes of less than a few keV ions were observed before the entry into the lobe. B_x decreased fairly abruptly at ≈1633 UT as the PS reappeared, B_z increased slightly and the magnetic intensity decreased, indicating the spacecraft was approaching the CS. After 1635 UT, the fluxes in the sunward and tailward directions were the same until ≈1645 UT, when a large mean velocity was observed. The spectrogram shows more ions travelling sunward than tailward in the ∼ 2-27 keV range, which resulted in a high mean velocity (∼600 km/s) in the sunward direction.

This event shows a low energy ion component that appeared immediately following the PS reappearance (∼1636 UT). Following the second increase of B_z (∼30 nT) at ∼1645 UT, in association with the large mean velocity, a large enhancement was observed. The absence of the low energy component between 1639-1645 is probably due to the fact that B_x was increasing, which indicates the spacecraft was moving further away from the CS. The low energy ion enhancement lasted for more than an hour, until ∼ 18 UT.

Figure 4 shows an example of the distribution taken at 1653:30 UT. As before, the ion distribution consisted of smooth, nearly isotropic contours for the high energy particles and a beam at ∼400 km/s propagating parallel to B. The electrons are anisotropic, $T_{||} > T_{\perp}$, with a weak field-aligned beam at -2×10^4 km/s propagating anti-parallel to B (away from the CS since negative B_x indicates that Wind is beneath the CS) and in the opposite direction from the ion beam. The 1D cuts show clearly that the distribution extends to low energies.

Summary and Discussion

We have shown that plasma distributions in the CS often consist of several distinct components. This in-

cludes the usual isotropic PS distribution, unidirectional and counter streaming ion beams with energies ≈1-3 keV, and low energy ions (few hundred eV). The concurrent electron distributions have bidirectional pitch-angle anisotropy (BPAA), counter streaming beams (not shown) and unidirectional beams that appear to be streaming away from the CS. These features have been observed in all of the first 26 Wind perigee passes. They all occur in association with substorm activity. The density contributed by the low energy ions can be as much as 40%.

Tailward streaming ion beams have been observed in the CPS region by Frank et al. (1996). The BPAA and counter streaming electron beams have been observed by Hada et al. (1981) at similar radial distances. Also, BPAA has been observed at radial distance of ∼70 R_e and further out by Geotail and referred to as flat-top electron distributions (Mukai et al., 1996). The counter streaming and earthward traveling ion beams and unidirectional electron beams we have shown here are new features in the CS, although similar electron beams have been observed near geosynchronous altitude (Johnstone et al., 1996). Frank et al. (1996) suggest that the tailward propagating ion beams originate in the ionosphere. Hada et al. (1981) suggest that BPAA are produced by the action of Fermi process due to high curvature of B near the CS and the counter-streaming electrons are of ionospheric origin.

Unidirectional electron beams are thought to be generated at the CS, because as exemplified by the three cases shown, they are always travelling away from the CS. This is indeed the case for all of the unidirectional electron beams observed by Wind 3DP (more than a hundred events studied). The farthest radial distance seen for these events is ∼30 R_e down in the tail. It's unlikely that these beams are from the ionosphere since even the asymmetry in the two hemispheres alone cannot account for this directional preferrence. To have the electron beams to be always propagating away from the CS, the asymmetry has to alternate in phase with the spacecraft location, that is, when Wind is in the northern hemisphere (above the CS), the asymmetry favors the southern hemisphere (beams are from the southern hemisphere); when Wind is in the southern hemisphere (below the CS), the asymmetry turns the other way.

The unidirectional ion and electron beams have similar energies, and we take this to mean the source of the ion beams could also be the CS. Analytical calculations have shown that electrons and ions are accelerated when interacting with the CS and ejected subsequently (see, for example, Lyons and Speiser, 1982; Zhu and

Parks, 1993). The counter-streaming ion beams could originate from the CS with the tailward going beam resulting from the mirroring of the earthward going beam. They could also come from conjugate ionospheres, but the beams have much wider pitch-angle spread than one would expect even if we take account of the finite aperture width. Hence, additional pitch-angle scattering process must be invoked to have taken place in transit for the source to be the ionosphere.

In conclusion, the plasma distribution in the tail CS is multicomponent, especially during geomagnetically active periods, thus a kinetic description of the dynamics is required.

Acknowledgments. The research at the University of Washington is supported in part by a NASA Grant NAG5-26850, and at Berkeley by NASA Grant NAG5-2815.

References

Akasofu, S.-I., Polar and Magnetospheric Substorm, Springer Verlag, New York, NY, 1968.

Frank, L. A., et al., Plasma velocity distributions in the near-Earth plasma sheet: A first look with the Geotail spacecraft, *J. Geophys. Res.*, *101*, 10627, 1996.

Hada, T., et al., Bi-directional electron pitch angle anisotropy in the plasma sheet, *J. Geophys. Res.*, *86*, 11211, 1981.

Johnstone, A. D., et al., Observations of particle injection from CRRES, Third International Conference on Substorms (ICS-3), 467, 1996.

Kokubun, S. and Y. Kamide, Substorms-4, Kluwer Academic Publishers, Dordrecht, Holland, 1998.

Lin, R. P., et al., A three dimensional plasma and energetic particle investigation for the Wind spacecraft, *Space Sci. Rev.*, *71*, 125, 1995.

Lui, A. T. Y. et al., Current Disruption in the Near Earth Neutral Sheet., *J. Geophys. Res.*, *97*, 1461, 1992.

Lyons, L. R. and T. W. Speiser, Evidence for current sheet acceleration in the neutral sheet., *J. Geophys. Res.*, *87*, 2276, 1982.

Mukai, T., et al., Structure and kinetic properties of plasmoids and their boundary regions., *J. Geomag. Geoelectr.*, *48*, 541, 1996.

Nakamura, M., et al., Ion distributions and flows near the neutral sheet, *J. Geophys. Res.*, *96*, 5631, 1991.

Parks, G. K. and J. R. Winckler, Substorm Electron Acceleration, *J. Geophys. Res.*, *73*, 5786, 1968.

Parks, G. K., et al., New observations of ion beams in the plasma sheet boundary layer, *Geophys. Res. Lett.*, *25*, 3285, 1998.

Zhu, Zhongwei and G. K. Parks, Particle orbits in model current sheet with a nonzero By component, *J. Geophys. Res.*, *98*, 7603, 1993.

L. Chen, M. McCarthy, and G. Parks, Geophysics Program, Box 351650, University of Washington, Seattle, WA 98195. (E-mail: lijen@u.washington.edu)

D. Larson and R. P. Lin, Space Science Laboratory, University of California, Berkeley, CA 94720

(Received September 17, 1999; revised November 9, 1999; accepted December 22, 1999.)

---

[1]Physics Department, University of Washington, Seattle, WA

[2]Geophysics Program, University of Washington, Seattle, WA

[3]Space Science Laboratory, University of California, Berkeley, CA

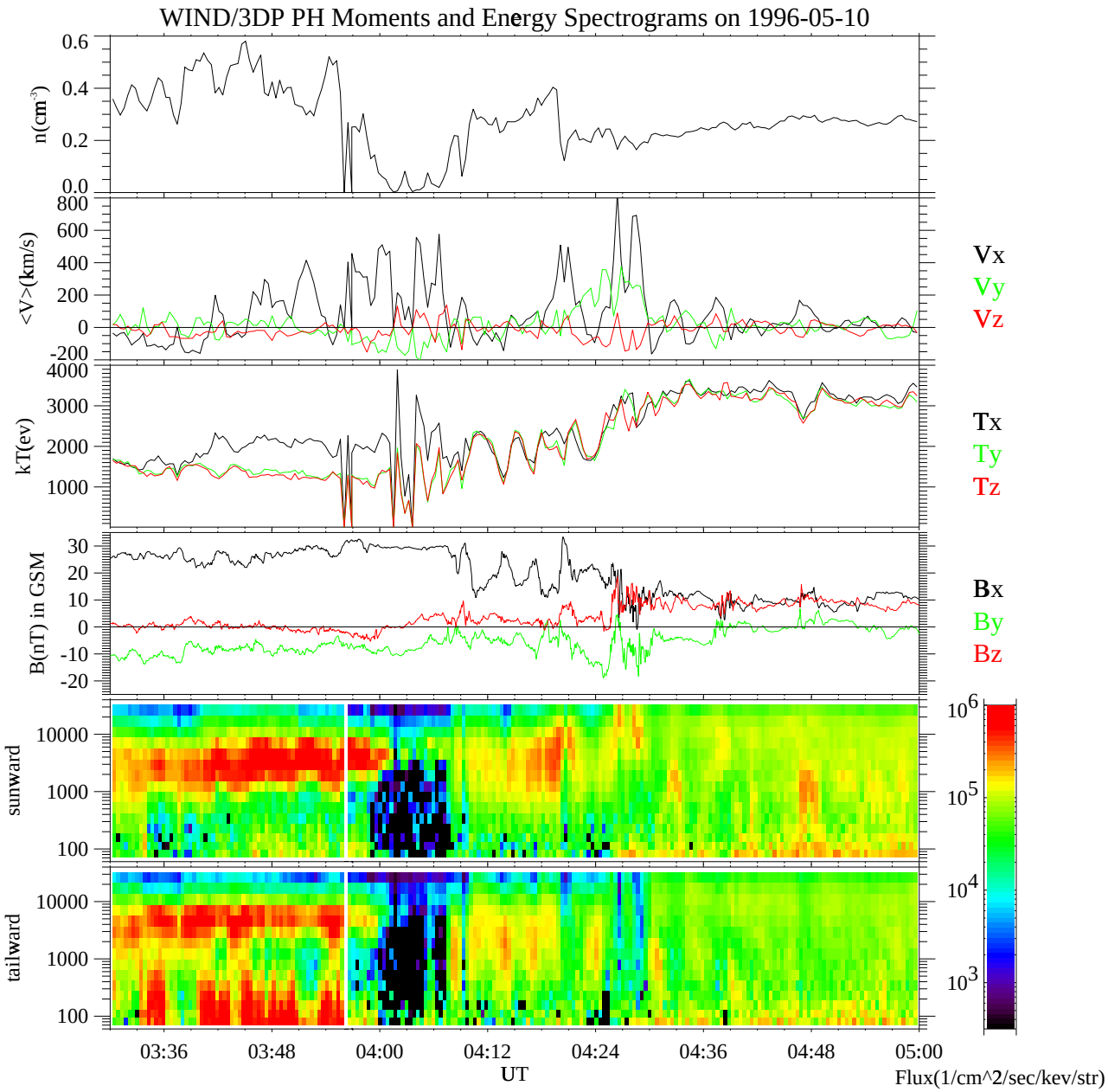

Figure 1. A summary plot of plasma activity observed on May 10, 1996 in the geomagnetic tail. See text for detailed explainations.

Figure 1. A summary plot of plasma activity observed on May 10, 1996 in the geomagnetic tail. See text for detailed explainations.

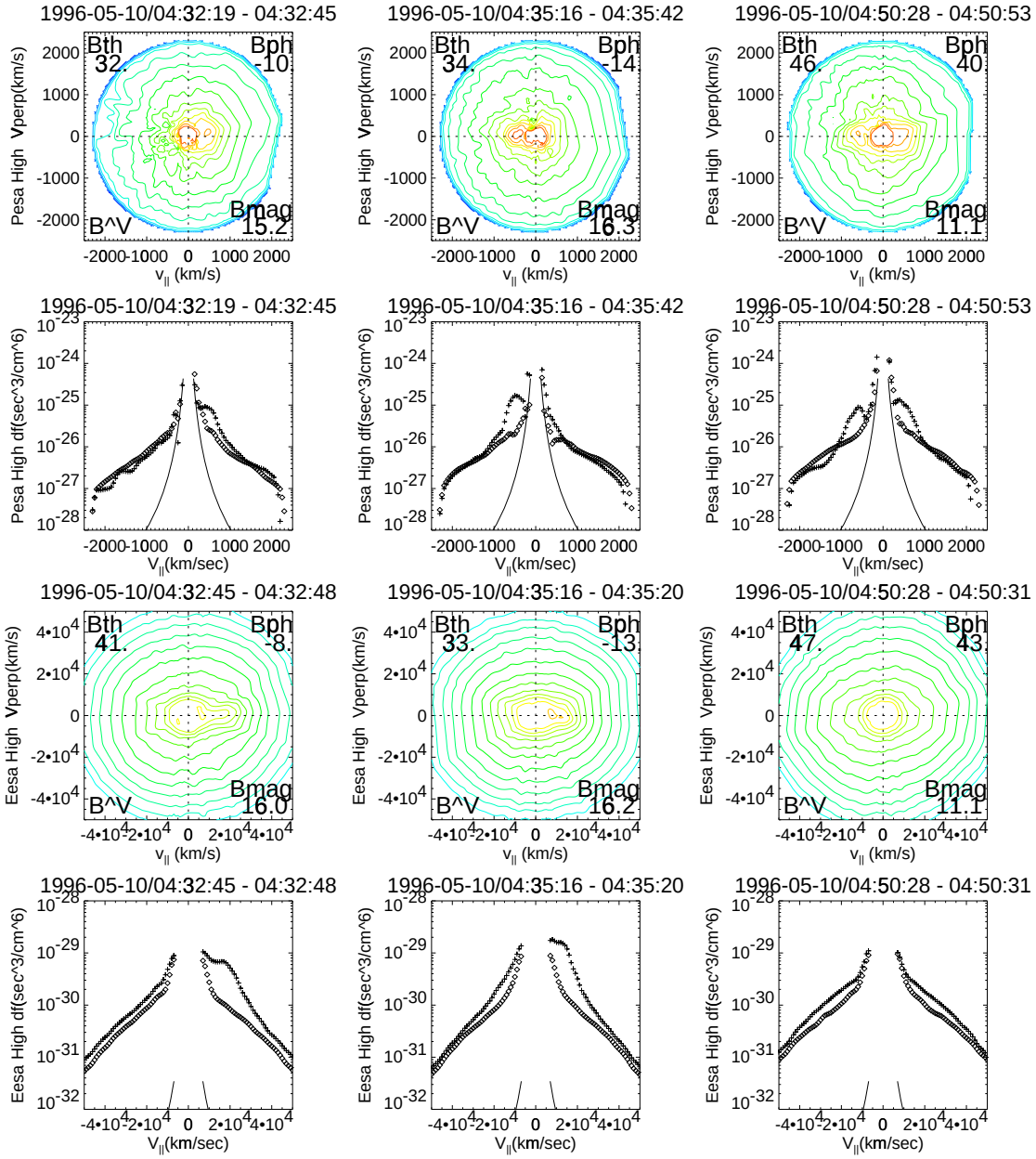

Figure 2. Isocontours of phase space density and 1D cuts of the ion and electron distributions in $(V_{||}, V_{\perp})$ space (see text for detailed explainations). Top two panels are for ions and bottom two are for electrons.

Figure 2. Isocontours of phase space density and 1D cuts of the ion and electron distributions in $(V_{||}, V_{\perp})$ space (see text for detailed explainations). Top two panels are for ions and bottom two are for electrons.

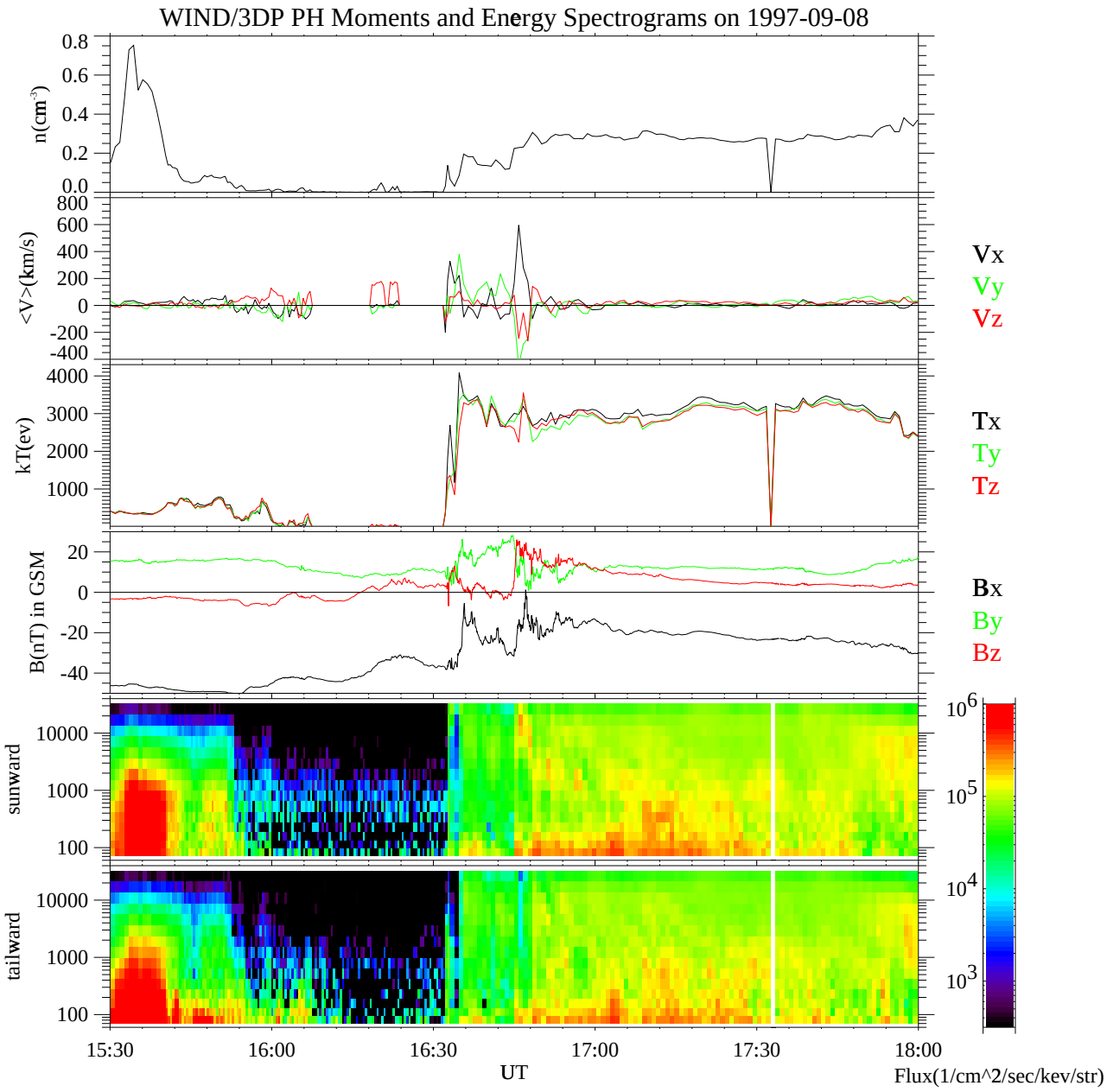

Figure 3. Another event displayed in the same format as Figure 1. The enhancement of low energy ions is preceeded by dramatic changes in the magnetic field, the keV ion beam and the unidirectional electron beam that is streaming away from the CS.

Figure 3. Another event displayed in the same format as Figure 1. The enhancement of low energy ions is preceeded by dramatic changes in the magnetic field, the keV ion beam and the unidirectional electron beam that is streaming away from the CS.

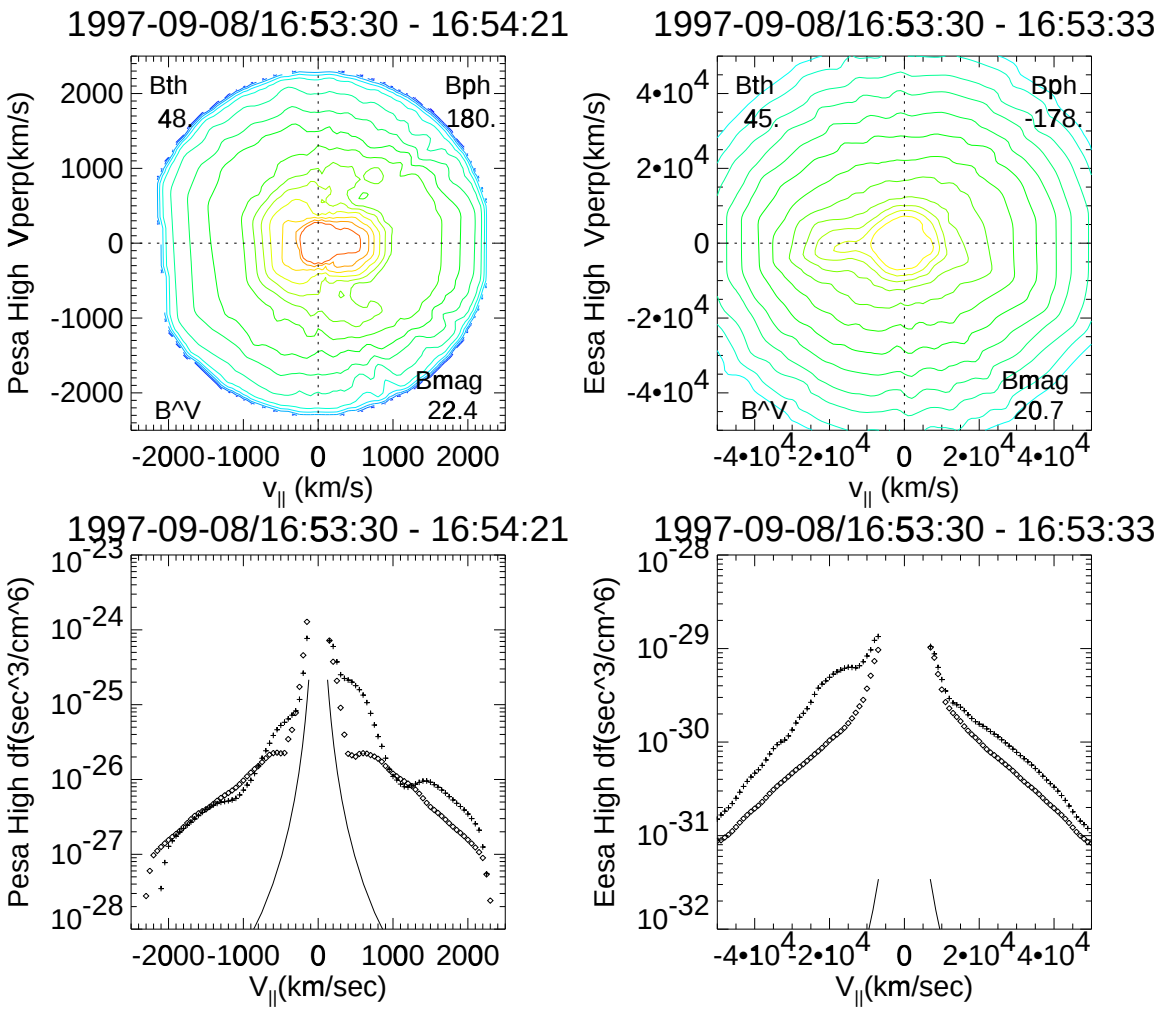

Figure 4. Ion (left two panels) and electron (right two panels) distributions displayed as isocontours of phase space density and 1D cuts of the distribution function. The format is similar to Figure 3. See text for detailed explainations.

Figure 4. Ion (left two panels) and electron (right two panels) distributions displayed as isocontours of phase space density and 1D cuts of the distribution function. The format is similar to Figure 3. See text for detailed explainations.

CHEN ET AL.: MULTICOMPONENT PLASMA IN THE CURRENT SHEET

CHEN ET AL.: MULTICOMPONENT PLASMA IN THE CURRENT SHEET

CHEN ET AL.: MULTICOMPONENT PLASMA IN THE CURRENT SHEET

CHEN ET AL.: MULTICOMPONENT PLASMA IN THE CURRENT SHEET

CHEN ET AL.: MULTICOMPONENT PLASMA IN THE CURRENT SHEET

CHEN ET AL.: MULTICOMPONENT PLASMA IN THE CURRENT SHEET

CHEN ET AL.: MULTICOMPONENT PLASMA IN THE CURRENT SHEET

CHEN ET AL.: MULTICOMPONENT PLASMA IN THE CURRENT SHEET

CHEN ET AL.: MULTICOMPONENT PLASMA IN THE CURRENT SHEET

CHEN ET AL.: MULTICOMPONENT PLASMA IN THE CURRENT SHEET

CHEN ET AL.: MULTICOMPONENT PLASMA IN THE CURRENT SHEET

CHEN ET AL.: MULTICOMPONENT PLASMA IN THE CURRENT SHEET

CHEN ET AL.: MULTICOMPONENT PLASMA IN THE CURRENT SHEET

CHEN ET AL.: MULTICOMPONENT PLASMA IN THE CURRENT SHEET

CHEN ET AL.: MULTICOMPONENT PLASMA IN THE CURRENT SHEET

CHEN ET AL.: MULTICOMPONENT PLASMA IN THE CURRENT SHEET

CHEN ET AL.: MULTICOMPONENT PLASMA IN THE CURRENT SHEET

CHEN ET AL.: MULTICOMPONENT PLASMA IN THE CURRENT SHEET

CHEN ET AL.: MULTICOMPONENT PLASMA IN THE CURRENT SHEET

CHEN ET AL.: MULTICOMPONENT PLASMA IN THE CURRENT SHEET

CHEN ET AL.: MULTICOMPONENT PLASMA IN THE CURRENT SHEET